Airborne observations of surface winds, waves and currents from meso to submesoscales

Luc Lenain[1], Benjamin K Smeltzer[2], Nicholas Pizzo[3], Mara A. Freilich[4], Luke Vincent Colosi[1], Simen ˚Adnøy Ellingsen[5], Laurent Grare[6], Hugo peyriere[1], and Nicholas M. Statom[7]

[1]Scripps Institution of Oceanography
[2]SINTEF
[3]Scripps Institution of Oceanography, UCSD
[4]UC San Diego
[5]Norwegian University of Science and Technology
[6]Scripps Institute of Oceanography
[7]University of California, San Diego

January 10, 2023

Abstract

In this work we present a unique set of coincident and collocated high- resolution observations of surface currents and directional properties of surface waves collected from an airborne instrument, the Modular Aerial Sensing System (MASS), collected off the coast of Southern California. High-resolution observations of near surface current profiles and shear are obtained using a new instrument, DoppVis, capable of capturing horizontal spatial current variability down to 128m resolution. This data set provides a unique opportunity to examine how currents at scales ranging from 1-100 km modulate bulk (e.g. significant wave height), directional and spectral properties of surface gravity waves. Such observations are a step toward developing better understanding of the underlying physics of submesoscale processes (e.g. frontogenesis and frontal arrest) and the nature of transitions between mesoscale and submesoscale dynamics.

Airborne observations of surface winds, waves and currents from meso to submesoscales

Luc Lenain[1*], Benjamin K. Smeltzer[2,3], Nick Pizzo[1], Mara Freilich[1,4], Luke Colosi[1], Simen Å. Ellingsen[2], Laurent Grare[1], Hugo Peyriere[1], and Nick Statom[1]

[1]Scripps Institution of Oceanography, University of California San Diego, La Jolla, CA 92037, USA
[2]Department of Energy Process Engineering, Norwegian University of Science and Technology, N-7491 Trondheim, Norway
[3]SINTEF Ocean, Marinteknisk senter, N-7052 Trondheim, Norway
[4]Department of Earth, Environmnetal and Planetary Science and Division of Applied Mathematics, Brown University, Providence, RI 02912, USA

Key Points:

- Unique coincident and collocated airborne observations of SST, surface currents and properties of surface waves across submesoscales features
- A new airborne instrument enables observations of surface currents, vertical and horizontal shear to capture quickly evolving ocean features
- Such observations are crucial to develop better understanding of the physics of submesoscale processes and wave-current interaction

*Corresponding author: Luc Lenain llenain@ucsd.edu

Abstract

In this work we present a unique set of coincident and collocated high- resolution observations of surface currents and directional properties of surface waves collected from an airborne instrument, the Modular Aerial Sensing System (MASS), collected off the coast of Southern California. High-resolution observations of near surface current profiles and shear are obtained using a new instrument, DoppVis, capable of capturing horizontal spatial current variability down to 128m resolution. This data set provides a unique opportunity to examine how currents at scales ranging from 1-100 km modulate bulk (e.g. significant wave height), directional and spectral properties of surface gravity waves. Such observations are a step toward developing better understanding of the underlying physics of submesoscale processes (e.g. frontogenesis and frontal arrest) and the nature of transitions between mesoscale and submesoscale dynamics.

Plain Language Summary

In recent years, through improvement of computational resolution of global ocean models, scientists have begun to suspect that kilometer-scale eddies, whirlpools and fronts, called “submesoscale” variability, make important contributions to horizontal and vertical exchange of climate and biological variables in the upper ocean. Such features are challenging to analyze, because of their size (and how quickly they evolve; within hours), they are too large to study from a research vessel but smaller than regions typically studied with satellite measurements. In this work, we use a research aircraft instrumented to characterize ocean currents, temperature, color (in turn chlorophyll concentration) and the properties of surface waves over an area large enough to capture submesoscale processes. This approach is a step forward in understanding and quantifying the underlying physics of submesoscale processes, and in turn develops parameterization that can help improve the fidelity of weather and climate models.

1 Introduction

The transfer of mass, momentum, and energy between the atmosphere and ocean are complex due to their interactions across a broad range of space and time scales (Melville, 1996). A better understanding of the physics of these processes is fundamental for improved parameterizations used in coupled air-sea models of weather and climate, particularly as Earth’s climate changes (Cavaleri et al., 2012). For example, although the importance of surface waves in these models has long been acknowledged, only relatively recently have global models included physics-based models of their effects (see, for example McWilliams & Restrepo, 1999; Sullivan & McWilliams, 2010; Li et al., 2016). Specifically, the effects of the non-breaking surface wave induced transport that catalyses Langmuir circulations have been shown to reduce errors in sea surface temperature (Belcher et al., 2012), crucial to climate modelling.

Submesoscale ocean currents have horizontal scales on the order of 0.1-10 km and have recently been hypothesized to make important contributions to vertical exchanges of climate and biological variables in the upper ocean as well as provide a pathway from energetically rich large scale flows to small scale dissipation. Model studies and limited observations (e.g. D’Asaro et al., 2018) show that submesoscale vertical exchange is concentrated near kilometer-scale fronts, jets, and eddies (McWilliams, 2016). Submesoscale physics are at the smallest scales that have been resolved in global ocean models, where their net effect on heat exchange between the ocean and atmosphere has shown to be much larger than mesoscale eddies (Su et al., 2018). However, these simulations are sensitive to the parameterized physics of the smaller scale motion, which remains poorly understood. To address the fundamental questions of the observed nature of submesoscale dynamics and the interactions between submesoscale dynamics and smaller scale surface wave processes, a comprehensive set of novel, coincident and collocated measurements of the dynamical variables is needed to improve state-of-the-art high-resolution simulations of weather and climate, and better understand vertical exchanges of heat and biogeochemical tracers.

Due to non-linear coupling between oceanic and atmospheric processes, including currents, winds, and waves, coincident observations are necessary to understand these dynamics. A number of model and observational studies have demonstrated the variety of ways by which air-sea interaction can induce horizontal divergence of surface currents and thus force vertical velocities. Coincident observations of surface vector winds and currents are needed to better understand the coupling of winds and currents and in turn improve surface flux parameterizations (Bourassa et al., 2019). The wind stress can be modified by SST and velocity gradients (Dewar & Flierl, 1987; Fairall et al., 1996; Chelton et al., 2004; O'Neill et al., 2005) while the resulting convergence of the ocean Ekman layer can be modified by surface vorticity (Stern, 1965; McGillicuddy Jr et al., 2007). At submesoscales, these effects are expected to increase in intensity. Frontal structures are strongly affected by the relative direction of the wind with *downfront* Ekman transport sharpening the fronts and inducing vertical exchange while *upfront* transport subdues the front and stratifies the upper ocean (Thomas et al., 2005). Surface waves and wave breaking can be strongly modulated at fronts (Romero et al., 2017; Vrećica et al., 2022), suggesting that even the basic formulation of air-sea exchange in terms of simple bulk coefficients will likely break down at sufficiently small scales. As such, an understanding of submesoscale structure and vertical velocity requires that air-sea interaction parameters be observed simultaneously with submesoscale measurements. Of particular interest are observations of surface and near surface currents, wave breaking (Vrećica et al., 2022), and the directional properties of ocean surface waves. While much progress have been made on characterizing the latter (e.g. Herbers et al., 2012; Lenain & Melville, 2014; Melville et al., 2016; Lenain & Melville, 2017; Lenain & Pizzo, 2020), collecting observations of near surface currents, i.e. from the surface down to several meters depth, remains challenging and spatially limited in large part due to the presence of waves, which induce platform motions and additional sources of background noise. An alternative approach to traditional in-situ techniques is to infer current profiles remotely based on observations of the spatio-temporal evolution of surface waves that follow a dispersion relationship, pursued in the present study.

In this work, we present a unique set of coincident and collocated observations of high-resolution surface currents and directional properties of surface waves collected from an airborne instrument, the Modular Aerial Sensing System (MASS), off the coast of Southern California in May 2021 as part of the ONR-funded Task Force Ocean (TFO) research initiative and in October 2021 as part of the NASA-funded Submesoscale Ocean Dynamics Experiment (S-MODE) research initiative. Two of the TFO research flights were dedicated to collecting observations across two small counter-rotating eddies separated by approximately 100 km. One of the S-MODE flights collected observations across a sharp SST front. This data set provides a unique opportunity to examine how currents at scales ranging from 1-100 km modulate surface gravity waves, i.e. bulk, directional and spectral properties.

This paper is structured as follows: the overview of the experiment and processing techniques is given in section 2 and 3. In sections 4 through 6, analysis of meso to submesoscales surface kinematics and currents collected during two experiments in Southern California is discussed. Section 7 discusses potential implications for submesoscale and air-sea interaction studies and presents some summary points.

2 Experiments

In this study we consider observations collected during two distinct experiments. The first was conducted as part of the "Platform Centric ASW Processing with Through-the-Sensor Data Assimilation and Fusion" project, funded through the ONR Task Force Ocean (TFO) initiative with the aim of collecting a simultaneous combination of acoustic, air-sea interaction and oceanographic measurements. Observations from a research vessel, a drifting instrument array, autonomous surface vehicles and a research aircraft were collected in May 2021, approximately 45km offshore of San Diego, CA, in the vicinity of CalCoFi Line #90.

The second experiment was conducted as part of the NASA S-MODE program, a project that aims to characterize the contribution of submesoscale ocean dynamics to vertical and horizontal transport in the upper ocean by employing a combination of aircraft-based remote sensing measurements of the ocean surface, in-situ measurements from research vessels and a variety of autonomous oceanographic platforms, and numerical modeling (Farrar et al., 2020). The "pilot" experiment considered here was conducted in the fall of 2021 off the coast of San Francisco, CA.

Data collected from instrumented Wave Gliders (Grare et al., 2021) and an airborne instrument, the SIO Modular Aerial Sensing System (MASS, Melville et al., 2016) during these two field programs are considered in the analysis. During both experiments the MASS instrument was installed on a Twin Otter DHC-6 aircraft (Twin Otter International, Grand Junction, CO).

3 SIO-MASS DoppVis instrument: Enabling novel airborne observations of near-surface currents

The Modular Aerial Sensing System (MASS) is an airborne instrument developed at the Air-Sea Interaction Laboratory (SIO) to simultaneously collect observations of sea surface temperature and ocean color (Melville et al., 2016; Lenain & Pizzo, 2021a), winds and mean-square slope (Lenain et al., 2019), surface waves (Lenain & Melville, 2017; Lenain & Pizzo, 2020), and ocean topography (Villas Bôas et al., 2022), at horizontal scales ranging from sub-meter to mesoscales. Over the past 11 years, the instrument was flown for more than 30 missions, covering a broad range of environmental conditions, locations, and applications. Details on the system performance and various applications of the MASS can be found in Melville et al. (2016); Lenain and Melville (2017); Lenain et al. (2019); Lenain and Pizzo (2020); Vrećica et al. (2022).

In 2020, we started the development and integration of a new sensor into the MASS instrument, called "DoppVis", to obtain coincident observations of surface currents alongside the MASS observations listed above. The approach used is to infer currents from optical observations of the spatio-temporal evolution of surface waves, whose dispersion is altered by the presence of an underlying current. This technique has been primarily used with radar technology (e.g. Stewart & Joy, 1974; Campana et al., 2016; Lund et al., 2015) then later applied to airborne video imagery (Dugan et al., 2001; Dugan & Piotrowski, 2003; Anderson et al., 2013).

Starting from the dispersion relation for small-amplitude linear waves propagating on top of a depth-varying current,

$$\omega(\mathbf{k}) = \omega_0(k) + \mathbf{c}(k) \cdot \mathbf{k}, \tag{1}$$

where ω is the wave frequency, ω_0 is the frequency in the absence of currents, i.e equal to $\sqrt{gk}$ in deep water, $\mathbf{k} = (k_x, k_y)$ is the wavenumber, $k = |\mathbf{k}|$, and $\mathbf{c}$ is the Doppler shift velocity due to the underlying current. Following Stewart and Joy (1974), assuming the waves are in deep-water, $\mathbf{c}$ can be approximated as a weighted average of the current profile as a function of depth such that

$$\mathbf{c}(k) = 2k \int_{-\infty}^{0} \mathbf{U}(z) e^{2kz} \mathrm{d}z, \tag{2}$$

where $\mathbf{U}(z) = (U, V)$ is the *Lagrangian* mean current profile as a function of depth z (Pizzo et al., 2022). Based on this relationship, one can assign an effective depth z_e to the measured Doppler velocities $\mathbf{c}(k)$ by finding the depth at which the Doppler velocity is equal to the current (Stewart & Joy, 1974; Smeltzer et al., 2019), such that $z_e(k) = -1/2k$. This is referred to as the Effective Depth Method (EDM) in Smeltzer et al. (2019).

The DoppVis instrument collects visible imagery of the ocean surface using a Nikon D850 camera with 14mm lens mounted with a 90 degree rotation (long edge of image parallel with flight track) and a 30 degree positive pitch angle from nadir (pointing slightly ahead of aircraft). The camera is synchronized to a coupled GPS/IMU system collecting images at a 2Hz frame rate. Raw images are carefully calibrated for lens distortion and boresight misalignment with the GPS/IMU over a hard terrestrial target, then georeferenced and exported with reference to WGS84 datum with a UTM zone 10 projection (EPSG 32610) at 50cm horizontal resolution. Each image is then interpolated on a regular grid, to enable the generation of 3D cubes of imagery (time, UTM X, UTM Y) of set duration and dimension (N_x, N_y), where $N_x = N_y$, typically in the range of 128 to 512m. The number of collected data cubes in the cross and along track direction of the aircraft varies as a function of aircraft altitude. All data presented here were collected at 1500 AMSL, corresponding to approximately two 256x256 m^2 cubes in the cross-track direction. Following the same approach described in (Smeltzer et al., 2019), all cubes of space–time data are converted to wavenumber–frequency space using a 3D FFT. Each of these 3D spectra are then averaged in the cross-track and along-track direction (1 km bin) to improve SNR. Doppler shift velocities are extracted from the spectrum as a function of wavenumber by masking the spectrum into wavenumber magnitude bins (bin half-width of $4\pi/N_x$), where for each bin the current $\mathbf{c}(k)$ is estimated using a normalized scalar product method (Huang et al., 2016; Streßer et al., 2017) with a Gaussian characteristic function (Smeltzer et al., 2019) peaked along the linear dispersion relation.

Figure 1(a) shows an example of current profiles (U, V) collected from DoppVis during an overflight of an instrumented Wave Glider during the S-MODE experiment on November 4, 2021 at 17:20 UTC. The Wave Glider was instrumented with an upward-looking Nortek Signature 1000 ADCP (orange squares) and a downward-looking ADCP (Teledyne RDI Workhorse 300kHz), carefully motion compensated using an onboard GPS/IMU system (Grare et al., 2021). Observations from DoppVis and the wave glider were collected within 5min and no further than 500m from each other to minimize any error associated with natural spatial and temporal variability. We find good agreement between in-situ and remotely sensed observations of near-surface current (U, V), with a bias = -0.014 m/s and rms deviation = 0.052 m/s, and a coefficient of determination $R^2 = 0.96$.

Finally, airborne observations of SST collected from MASS on November 4, 2021, over the entire domain along with current estimates (1km along-track resolution) from DoppVis at two depths, $z = -1.5 \pm 0.5$m (black arrows) and $z = -0.4 \pm 0.1$m (red arrows) are shown in figure 1(c). Note the correlation between features present in the SST fields and the surface currents from DoppVis. Throughout the domain, we consistently find larger magnitudes of the eastern component of the current closer to the surface, likely caused by Stokes drift included in the Lagrangian current observed by DoppVis (Pizzo et al., 2022). Wind and waves were coming from the west at the time of the flight.

4 Wave-current interactions from meso- to submesoscales

The collocated observations from the multiple instruments on the MASS allow for investigation of interactions between currents and other oceanographic properties such as waves, heat, and biological communities. We now examine observations collected during the "Platform Centric ASW Processing with Through-the-Sensor Data Assimilation and Fusion" TFO project in May 2021 to illustrate the importance of high spatial resolution, collocated observations for studying wave-current observations.

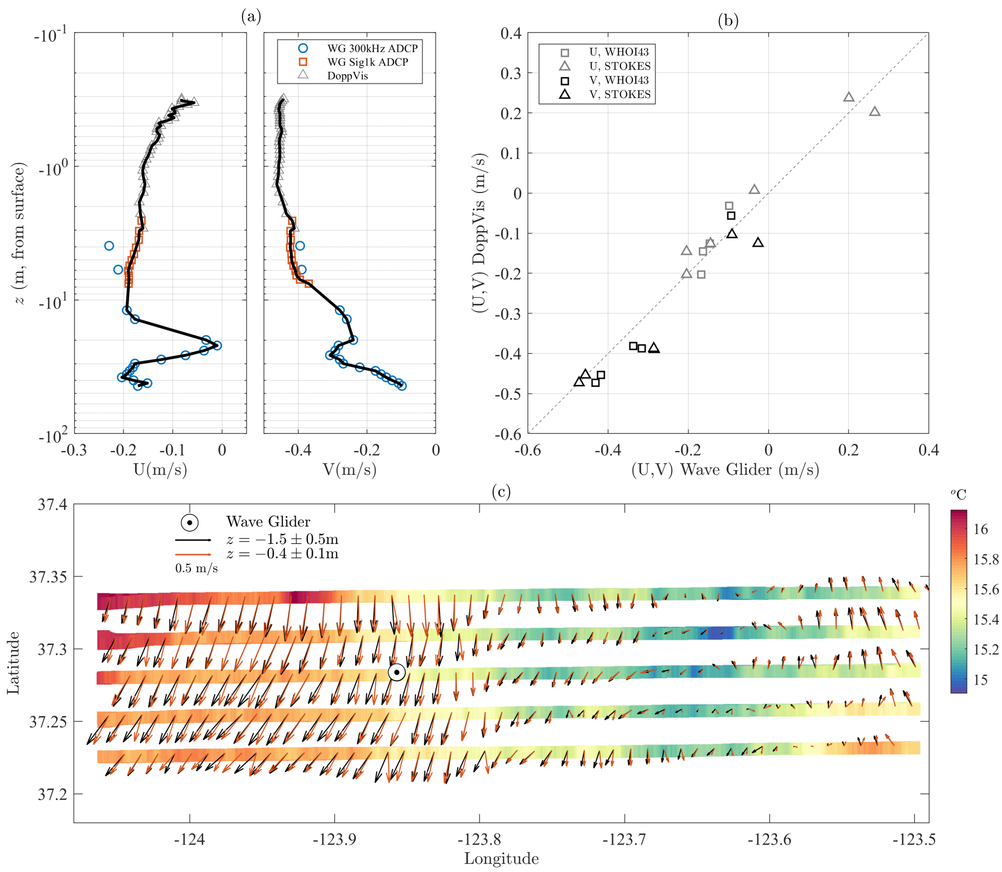

Figure 1. (a) Current profiles (U, V) collected from DoppVis (gray triangles) during an overflight of an instrumented Wave Glider during the S-MODE experiment on November 4, 2021 at 17:20 UTC. The Wave Glider is equipped with an upward-looking Nortek Signature 1000 ADCP (orange squares) and a downward-looking ADCP (Teledyne RDI Workhorse 300kHz; blue circles). The location of the Wave Glider with respect to the DoppVis observations is shown in (c). (b) Comparison between in-situ observations of currents collected at a 2 to 3m water depth obtained from DoppVis and two Wave Gliders, named WHOI43 and STOKES, for the times and locations of overflights (within 500m) during the entire S-MODE experiment. (c) Airborne observations of SST collected from MASS on November 4, 2021 over the entire domain along with current estimates (1km along-track resolution) from DoppVis at two depths, deep, $z = -1.5 \pm 0.5$m (black arrows) and shallow, $z = -0.4 \pm 0.1$m (red arrows).

Several research flights were dedicated to collecting observations across two counter-rotating eddies separated by approximately 100 km. Figure 2(a) shows depth-averaged (0.3-2m) surface currents (250 m along-track resolution) along with significant wave height measurements collected coincidentally with the MASS instrument. The black contours represent the sea surface height (ssh, AVISO) at the time of the observations, while corresponding surface currents from HYCOM (GOF 3.1, GLBy0.08-expt93.0) are shown as gray quivers. We find the HYCOM estimated currents to be in good agreement with DoppVis observations at the mesoscale, but strikingly miss many of the submesoscale features throughout the domain. We also find significant modulation of the surface wave properties across the domain that is not caused by temporal (e.g. inertial) variability.

Currents modulate the properties of surface gravity waves both through wave refraction (e.g. Ardhuin et al., 2017; Romero et al., 2017, 2020; Bôas et al., 2020; Pizzo & Salmon, 2021) and local effects (Rascle et al., 2016, 2017; Lenain & Pizzo, 2021b), therefore high-resolution measurements of currents and spectral wave properties is needed to better understand wave-current interaction from meso- to submesoscales.

Figure 2 shows a subset of these observations, focusing on an area of the domain with significant submesoscale variability in ocean current magnitude and direction. We find large modulation of surface currents, at scales of 1-8 km associated with submesoscale variations within the mesoscale eddy. Panel (b) shows a sharp SST front at 32.885^{o}N with a change in temperature of approximately 0.5^oC, associated with a velocity gradient $\partial U/\partial x \approx 10f$, where f is the Coriolis frequency.

Despite approximately constant surface wind (figure 2c) and significant wave height (figure 2d) as a function of latitude on this transect, the mean spectral saturation $< B >$ (Romero et al., 2017) had significant variation (figure 2e). The saturation spectrum is defined as $B = \phi(k)k^3$, where ϕ is the omnidirectional wave spectrum (Phillips, 1984, 1985). The mean saturation is obtained by averaging B over the saturation range of the wave spectrum, with a lower bound k_n as defined in Lenain and Pizzo (2020). At that time, wind waves were approximately oriented in the same direction as the current V (figure 2d).

We find that the mean saturation $< B >$ generally follow the same evolution as V. While this comparison remains qualitative, it hints at the importance of incorporating wave-current interaction in wave spectrum parameterization, along the line of Lenain and Pizzo (2021a) that investigated the use of WKB to predict the modulation of surface gravity waves by internal wave currents.

Though beyond the scope of this work, but a focus of further studies in particular as part of the S-MODE program, we expect that these collocated, coincident observations will lead to new insights about coherent features that arise from wind-wave-current coupling, or some combination of those processes, which may be particularly important for the flux of climatically-important variables such as heat and biogeochemical tracers between atmosphere and ocean (Li et al., 2016; Smith et al., 2016; Verma & Sarkar, 2021; Freilich & Mahadevan, 2021; Gula et al., 2022).

5 Transitions from mesoscale to submesoscale motion

High-resolution measurements of surface currents enable the characterization of the transition between geostrophically balanced motion at larger scales and unbalanced (ageostrophic and wave) motion at smaller scales (Chereskin et al., 2019). In particular, determining the dynamics that predominate at the submesoscale has important implications for the vertical structure of the upper-ocean (Cronin et al., 2019) and the spatio-temporal distribution of energy dissipation (Buckingham et al., 2019; Dong et al., 2020; Schubert et al., 2020; Ajayi et al., 2021), and can lead to improvement of ocean-atmosphere coupled models (Li et al., 2016). While DoppVis observations are accurate enough to resolve sub-

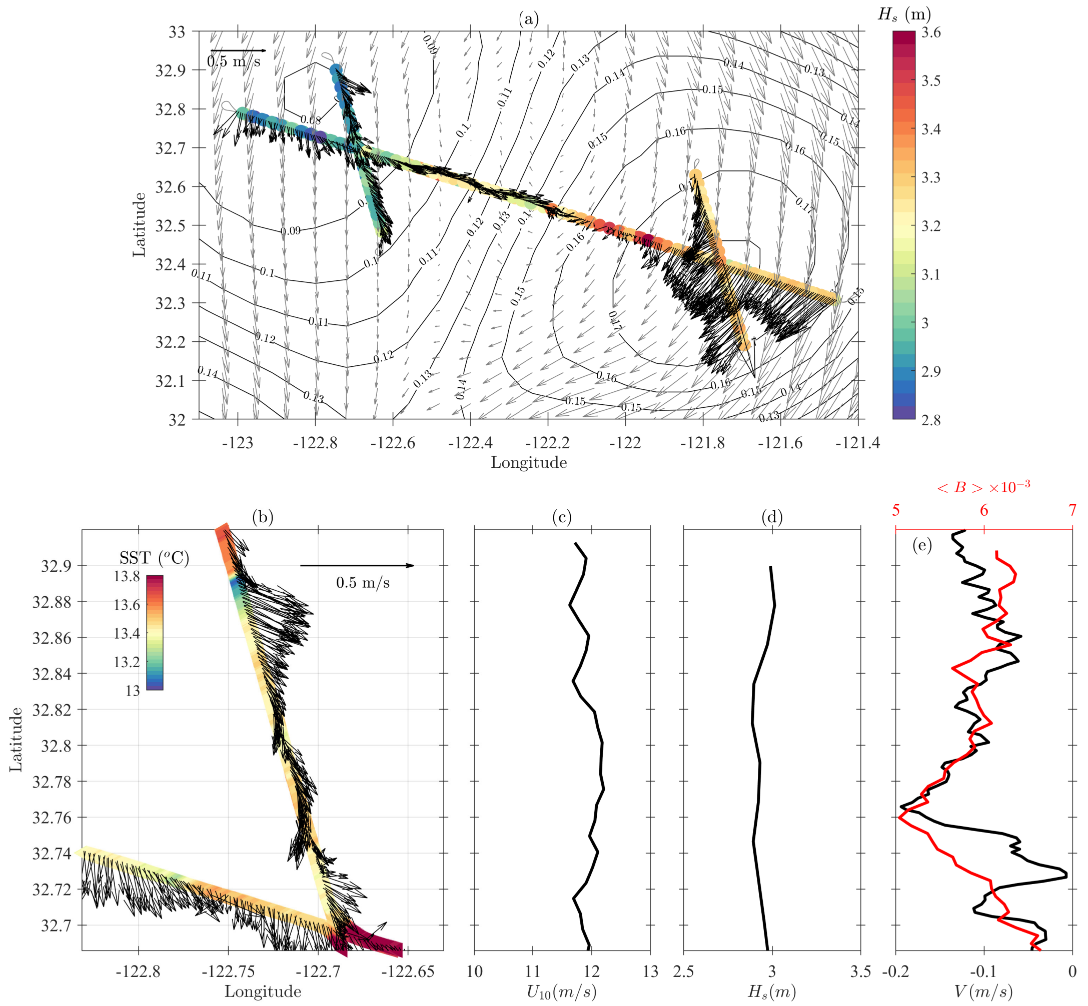

Figure 2. (a) MASS significant wave height H_s and DoppVis surface current observations (250m along-track resolution) collected during the TFO experiment on May 19, 2021. The black contours represent the sea surface height (ssh, AVISO) at the time of the observations, while corresponding surface currents from HYCOM are shown as gray quivers. The larger scale trends of the surface currents are in general agreement with the HYCOM product, though the latter completely misses significant submesoscale features. We find significant modulation of the wave conditions across the domain, by up to 20%. (b) Subset of the data presented in (a) (nortwestern part of the flight) with the track colorcoded for measured SST. Note the strong modulation of surface currents over very short distances (1-8 km), coinciding in places with sharp SST fronts (for example at latitude around 32.885^o in the northern part of the operation area). (c) and (d) show the wind speed U_{10} and significant wave height H_s collected along the NNW-SSE track shown in panel (b). (e) North component of the current V and mean spectral saturation $\langle B \rangle$, all plotted over the same range of latitude as in panel (b). Note the modulation of $\langle B \rangle$ associated with changes in V, the component of the current aligned with the waves, hinting at local wave-current interaction.

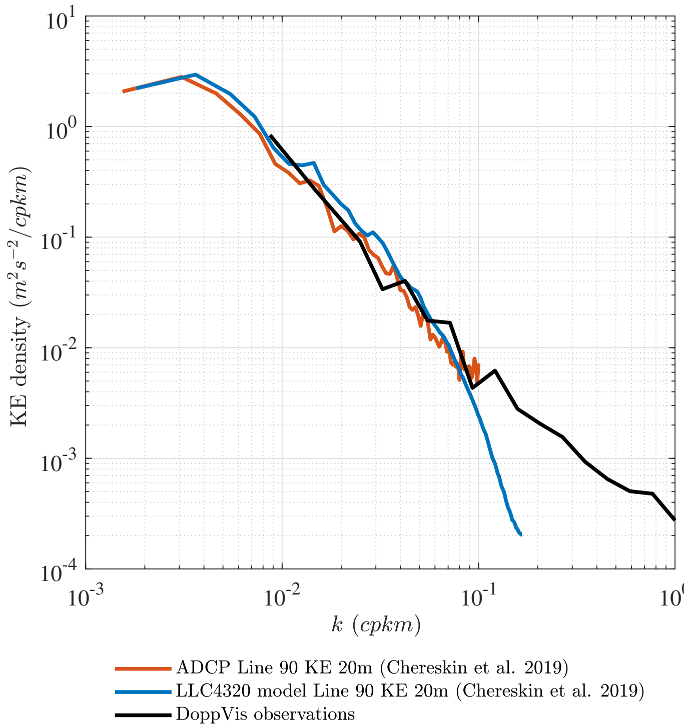

Figure 3. Comparison of Kinetic energy (KE) spectra collected from the DoppVis Lagrangian surface currents on May 19 2021 during one of the long East - West transects shown in figure 2(a) compared with in-situ ADCP observations (20-m depth) and LLC4320 hourly model products from Chereskin et al. (2019).

mesoscale currents (horizontal resolution of less than 500 m), the airborne platform also travels quickly enough to collect nearly synoptic observations at the mesoscale (100 km). This is particularly valuable because it allows for examination of spatial variability across a range of scales and cross-scale interactions by not aliasing temporal variability. Figure 3 shows kinetic energy (KE) spectra computed from the DoppVis surface current observations collected during one of the long East-West transects shown in figure 2(a) compared with the average of 11 years of in-situ ADCP observations (20-m depth) and 1 year of LLC4320 hourly model products from Chereskin et al. (2019). The agreement at low wavenumbers (>10km) is remarkable, as well as the fact that the kinetic energy spectrum from DoppVis maintains a nearly continuous slope for higher wavenumbers, down to 1 km scale. Feedbacks on ocean currents from wind and waves is likely important for determining dynamics at scales of less than 10 km where submesoscale processes predominate (Haney et al., 2015; Suzuki & Fox-Kemper, 2016; Yuan & Liang, 2021). Understanding these couplings needs to be advanced by direct observations that span scales from submesoscale to mesoscale. Characterization of the transition between geostrophically balanced motion and unbalanced dynamics is further explored in forthcoming work.

6 Velocity gradient statistics

Submesoscale dynamics are defined by the large velocity gradients at these scales, with $\mathcal{O}(1)$ Rossby number (McWilliams, 2016). Consistent with the small spatial scale of submesoscale dynamics, they also have fast temporal scales (Callies et al., 2020). Observations of not just velocity, but 2D velocity gradients of quickly evolving submesoscale features are therefore important for understanding submesoscale dynamics, but require

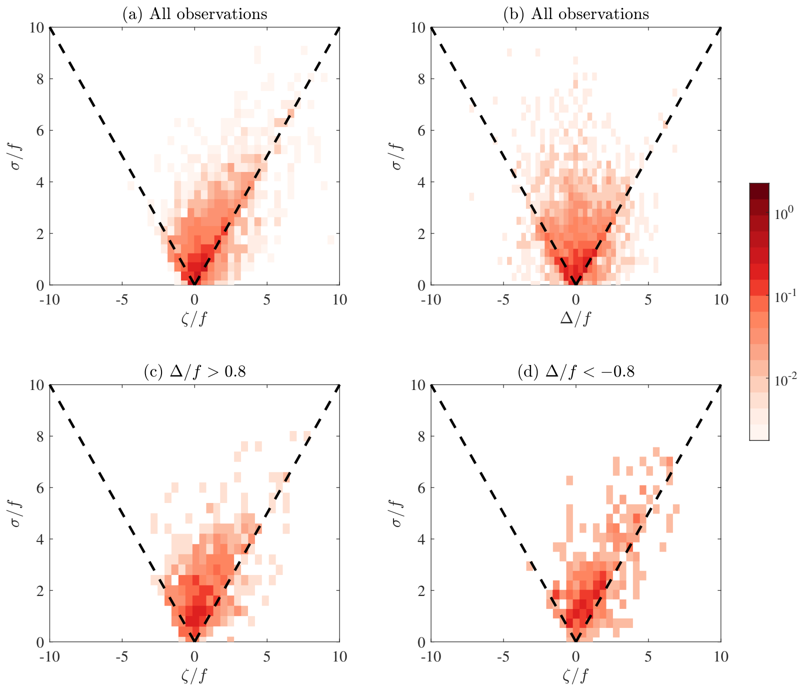

Figure 4. (a) Surface vorticity–strain and (b) divergence-strain JPDFs computed from 128m resolution DoppVis products collected on October 5 2021 during the S-MODE pilot program. (c) and (d) Surface vorticity–strain for $\Delta/f > 0.8$ and $\Delta/f < -0.8$ respectively. The dashed lines represents the $\sigma = \zeta$ lines.

synoptic observations over scales of tens of kilometers, which is not feasible with relatively slow-moving ship-based observations. Previous observations of submesoscale velocity gradients have used two ships (Shcherbina et al., 2013). Aircraft-based observations offer a well-suited platform for studying submesoscale dynamics due to their fast speed relative to ships and much higher resolution measurements than what is afforded by satellites.

In recent years, through numerical (Balwada et al., 2021) and observational (Shcherbina et al., 2013) studies, the surface vorticity–strain Joint Probability Density Function (JPDF) has been demonstrated as a useful tool to distinguish between different flow regimes, in particular in the context of submesoscale dynamics. In figure 4, we show vorticity-strain and divergence-strain JPDFs computed from high-resolution DoppVis surface current observations collected during the S-MODE pilot experiment on October 2021 (60km long section). During that portion of the flight, the aircraft flew at 3000ft AMSL, increasing the swath width of surface current observation up to 2 km, with a horizontal resolution (cross and along-track) of 128 m. Vorticity ζ, strain rate σ and divergence Δ are then computed from the gradients of the measured surface currents. These velocities are first low-pass filtered (3-point tophat) prior to computing gradients. Overall, the distribution is skewed toward positive ζ/f values, with $\sigma/f > \zeta/f$ consistent with frontal structures, and classical submesoscale frontogenesis. This is particularly evident in panel (d), where the vorticity-strain JPDF for $\Delta/f < -0.8$ (i.e. convergence) is shown to be skewed to positive values. The same JPDF for positive values of Δ/f, larger than 0.8 (panel c) is not skewed toward negative ζ/f values, perhaps implying the contribution of other processes, e.g. surface wave modulation properties and associated Stokes drift (recall that DoppVis observes Lagrangian current).

7 Discussions and summary

Direct spatial and temporal observations of the lower atmosphere, sea surface and upper ocean are crucial for improved knowledge of air-sea interaction. However, the broad range of scales, or equivalently the strong spatial and temporal variability of theses interactions (see figure 1), make this a formidable theoretical, numerical, and observational challenge. Traditional in-situ assets such as moorings and buoys are limited by their spatial coverage or their potential spatial biasing, in particular near an ocean front where buoys or drifters can cluster, while satellite imagery estimates important quantities like wind, significant wave height and currents through indirect methods (often based on σ_0 relations) and can also only sample at sparse time intervals. Observations and models have revealed two-way coupling processes between ocean currents and wind (Chelton & Xie, 2010; Wenegrat & Arthur, 2018) and ocean currents and waves (Marechal & de Marez, 2022; Wang et al., 2020) at both the mesoscale and submesoscale.

In this work, we present unique coincident and collocated suborbital high-resolution observations of SST, surface currents and directional properties of surface waves collected from an airborne instrument (MASS), off the coast of Southern California, across submesoscales features.

Central to this work is the development of a novel airborne instrument, DoppVis, that enables high-resolution observations of surface currents, vertical and horizontal shear alongside the other MASS instruments to capture quickly evolving features (both in time and space) such as submesoscale fronts, but also tidal estuarine flows, and more generally ocean phenomena that require frequent revisits (e.g oil spills).

The combination of surface waves, currents, and SST remotely observed from this instrument provides a unique opportunity to examine how currents at scales ranging from 1-100 km modulate surface gravity waves, i.e. bulk (e.g. significant wave height), directional and spectral properties. Observations of near-surface currents at such high spatial resolution also enable the investigation of the transition between balanced and unbalanced motion, and the flow structure (vorticity-strain space), crucial to developing a better understanding of the underlying physics of submesoscale processes such as frontogenesis and frontal arrest.

Acknowledgments

We gratefully acknowledge useful comments from Ernesto Rodriguez and Roy Barkan. The authors are grateful to Twin Otter International for providing flight resources. This research was supported by grants from the Physical Oceanography programs at ONR (Grant N00014-19-1-2635), and NASA (Grant 80NSSC19K1688).

Open research

Data availability: All presented data will be found at the UCSD Library Digital Collection, https://doi.org/10.6075/J0F76CRK (data archiving is underway).

References

Ajayi, A., Le Sommer, J., Chassignet, E. P., Molines, J.-M., Xu, X., Albert, A., & Dewar, W. (2021). Diagnosing cross-scale kinetic energy exchanges from two submesoscale permitting ocean models. *Journal of Advances in Modeling Earth Systems*, *13*(6), e2019MS001923.

Anderson, S. P., Zuckerman, S., Fan, S., & van Smirren, J. (2013). Airborne optical remote sensing of ocean currents. In *2013 oceans-san diego* (pp. 1–7).

Ardhuin, F., Gille, S. T., Menemenlis, D., Rocha, C. B., Rascle, N., Chapron, B.,

… Molemaker, J. (2017). Small-scale open ocean currents have large effects on wind wave heights. *Journal of Geophysical Research: Oceans*, *122*(6), 4500–4517.

Balwada, D., Xiao, Q., Smith, S., Abernathey, R., & Gray, A. R. (2021). Vertical fluxes conditioned on vorticity and strain reveal submesoscale ventilation. *Journal of Physical Oceanography*, *51*(9), 2883–2901.

Belcher, S. E., Grant, A. L., Hanley, K. E., Fox-Kemper, B., Van Roekel, L., Sullivan, P. P., … others (2012). A global perspective on langmuir turbulence in the ocean surface boundary layer. *Geophysical Research Letters*, *39*(18).

Bôas, A. B. V., Cornuelle, B. D., Mazloff, M. R., Gille, S. T., & Ardhuin, F. (2020). Wave–current interactions at meso-and submesoscales: Insights from idealized numerical simulations. *Journal of Physical Oceanography*, *50*(12), 3483–3500.

Bourassa, M. A., Meissner, T., Cerovecki, I., Chang, P. S., Dong, X., De Chiara, G., … others (2019). Remotely sensed winds and wind stresses for marine forecasting and ocean modeling. *Frontiers in Marine Science*, 443.

Buckingham, C. E., Lucas, N. S., Belcher, S. E., Rippeth, T. P., Grant, A. L., Le Sommer, J., … Naveira Garabato, A. C. (2019). The contribution of surface and submesoscale processes to turbulence in the open ocean surface boundary layer. *Journal of Advances in Modeling Earth Systems*, *11*(12), 4066–4094.

Callies, J., Barkan, R., & Garabato, A. N. (2020). Time scales of submesoscale flow inferred from a mooring array. *Journal of Physical Oceanography*, *50*(4), 1065–1086.

Campana, J., Terrill, E. J., & De Paolo, T. (2016). The development of an inversion technique to extract vertical current profiles from x-band radar observations. *Journal of Atmospheric and Oceanic Technology*, *33*(9), 2015–2028.

Cavaleri, L., Fox-Kemper, B., & Hemer, M. (2012). Wind waves in the coupled climate system. *Bulletin of the American Meteorological Society*, *93*(11), 1651–1661.

Chelton, D. B., Schlax, M. G., Freilich, M. H., & Milliff, R. F. (2004). Satellite measurements reveal persistent small-scale features in ocean winds. *science*, *303*(5660), 978–983.

Chelton, D. B., & Xie, S.-P. (2010). Coupled ocean-atmosphere interaction at oceanic mesoscales. *Oceanography*, *23*(4), 52–69.

Chereskin, T. K., Rocha, C. B., Gille, S. T., Menemenlis, D., & Passaro, M. (2019). Characterizing the transition from balanced to unbalanced motions in the southern california current. *Journal of Geophysical Research: Oceans*, *124*(3), 2088–2109.

Cronin, M. F., Gentemann, C. L., Edson, J., Ueki, I., Bourassa, M., Brown, S., … others (2019). Air-sea fluxes with a focus on heat and momentum. *Frontiers in Marine Science*, *6*, 430.

Dewar, W. K., & Flierl, G. R. (1987). Some effects of the wind on rings. *Journal of physical oceanography*, *17*(10), 1653–1667.

Dong, J., Fox-Kemper, B., Zhang, H., & Dong, C. (2020). The seasonality of submesoscale energy production, content, and cascade. *Geophysical Research Letters*, *47*(6), e2020GL087388.

Dugan, J., & Piotrowski, C. (2003). Surface current measurements using airborne visible image time series. *Remote Sensing of Environment*, *84*(2), 309–319.

Dugan, J., Piotrowski, C., & Williams, J. (2001). Water depth and surface current retrievals from airborne optical measurements of surface gravity wave dispersion. *Journal of Geophysical Research: Oceans*, *106*(C8), 16903–16915.

D'Asaro, E. A., Shcherbina, A. Y., Klymak, J. M., Molemaker, J., Novelli, G., Guigand, C. M., … others (2018). Ocean convergence and the dispersion of flotsam. *Proceedings of the National Academy of Sciences*, *115*(6), 1162–1167.

Fairall, C. W., Bradley, E. F., Rogers, D. P., Edson, J. B., & Young, G. S. (1996). Bulk parameterization of air-sea fluxes for tropical ocean-global atmosphere coupled-ocean atmosphere response experiment. *Journal of Geophysical Research: Oceans*, *101*(C2), 3747–3764.

Farrar, J. T., D'Asaro, E., Rodriguez, E., Shcherbina, A., Czech, E., Matthias, P., ... others (2020). S-mode: The sub-mesoscale ocean dynamics experiment. In *Igarss 2020-2020 ieee international geoscience and remote sensing symposium* (pp. 3533–3536).

Freilich, M., & Mahadevan, A. (2021). Coherent pathways for subduction from the surface mixed layer at ocean fronts. *Journal of Geophysical Research: Oceans*, *126*(5), e2020JC017042.

Grare, L., Statom, N. M., Pizzo, N., & Lenain, L. (2021). Instrumented wave gliders for air-sea interaction and upper ocean research. *Frontiers in Marine Science*, 888.

Gula, J., Taylor, J., Shcherbina, A., & Mahadevan, A. (2022). Submesoscale processes and mixing. In *Ocean mixing* (pp. 181–214). Elsevier.

Haney, S., Fox-Kemper, B., Julien, K., & Webb, A. (2015). Symmetric and geostrophic instabilities in the wave-forced ocean mixed layer. *Journal of Physical Oceanography*, *45*(12), 3033–3056.

Herbers, T. H. C., Jessen, P. F., Janssen, T. T., Colbert, D. B., & MacMahan, J. H. (2012). Observing ocean surface waves with gps-tracked buoys. *J. Atmos. Oceanic Technol.*, *29*, 944–959.

Huang, W., Carrasco, R., Shen, C., Gill, E. W., & Horstmann, J. (2016). Surface current measurements using x-band marine radar with vertical polarization. *IEEE Transactions on Geoscience and Remote Sensing*, *54*(5), 2988–2997.

Lenain, L., & Melville, W. K. (2014). Autonomous surface vehicle measurements of the ocean's response to tropical cyclone freda. *Journal of Atmospheric and Oceanic Technology*, *31*(10), 2169–2190.

Lenain, L., & Melville, W. K. (2017). Measurements of the directional spectrum across the equilibrium saturation ranges of wind-generated surface waves. *Journal of Physical Oceanography*, *47*(8), 2123–2138.

Lenain, L., & Pizzo, N. (2020, 09). The contribution of high frequency wind-generated surface waves to the Stokes drift. *Journal of Physical Oceanography*, 1-39. Retrieved from `https://doi.org/10.1175/JPO-D-20-0116.1` doi: 10.1175/JPO-D-20-0116.1

Lenain, L., & Pizzo, N. (2021a). Modulation of surface gravity waves by internal waves. *Journal of Physical Oceanography*, *51*(9), 2735–2748.

Lenain, L., & Pizzo, N. (2021b). Modulation of surface gravity waves by internal waves. *Journal of Physical Oceanography*, *51*(9), 2735–2748.

Lenain, L., Statom, N. M., & Melville, W. K. (2019). Airborne measurements of surface wind and slope statistics over the ocean. *Journal of Physical Oceanography*(2019).

Li, Q., Webb, A., Fox-Kemper, B., Craig, A., Danabasoglu, G., Large, W. G., & Vertenstein, M. (2016). Langmuir mixing effects on global climate: Wavewatch iii in cesm. *Ocean Modelling*, *103*, 145–160.

Lund, B., Graber, H. C., Tamura, H., Collins III, C., & Varlamov, S. (2015). A new technique for the retrieval of near-surface vertical current shear from marine x-band radar images. *Journal of Geophysical Research: Oceans*, *120*(12), 8466–8486.

Marechal, G., & de Marez, C. (2022). Variability of surface gravity wave field over a realistic cyclonic eddy. *Ocean Science*, *18*(5), 1275–1292.

McGillicuddy Jr, D. J., Anderson, L. A., Bates, N. R., Bibby, T., Buesseler, K. O., Carlson, C. A., ... others (2007). Eddy/wind interactions stimulate extraordinary mid-ocean plankton blooms. *Science*, *316*(5827), 1021–1026.

McWilliams, J. C. (2016). Submesoscale currents in the ocean. *Proceedings of the*

Royal Society A: Mathematical, Physical and Engineering Sciences, *472*(2189), 20160117.

McWilliams, J. C., & Restrepo, J. M. (1999). The wave-driven ocean circulation. *Journal of Physical Oceanography*, *29*(10), 2523–2540.

Melville, W. K. (1996). The role of surface wave breaking in air-sea interaction. *Annual Review of Fluid Mechanics*, *28*, 279-321.

Melville, W. K., Lenain, L., Cayan, D. R., Kahru, M., Kleissl, J. P., Linden, P., & Statom, N. M. (2016). The modular aerial sensing system. *Journal of Atmospheric and Oceanic Technology*, *33*(6), 1169–1184.

O'Neill, L. W., Chelton, D. B., Esbensen, S. K., & Wentz, F. J. (2005). High-resolution satellite measurements of the atmospheric boundary layer response to sst variations along the agulhas return current. *Journal of Climate*, *18*(14), 2706 - 2723. doi: 10.1175/JCLI3415.1

Phillips, O. (1984). On the response of short ocean wave components at a fixed wavenumber to ocean current variations. *Journal of Physical Oceanography*, *14*(9), 1425–1433.

Phillips, O. (1985). Spectral and statistical properties of the equilibrium range in wind-generated gravity waves. *Journal of Fluid Mechanics*, *156*(1), 505–31.

Pizzo, N., Lenain, L., Romcke, O., Ellingsen, O., & Smeltzer, B. (2022). The role of lagrangian drift in the geometry, kinematics and dynamics of surface waves. *Journal of Fluid Mechanics*, *Sub Judice*.

Pizzo, N., & Salmon, R. (2021). Particle description of the interaction between wave packets and point vortices. *Journal of Fluid Mechanics*, *925*.

Rascle, N., Molemaker, J., Marié, L., Nouguier, F., Chapron, B., Lund, B., & Mouche, A. (2017). Intense deformation field at oceanic front inferred from directional sea surface roughness observations. *Geophysical Research Letters*, *44*(11), 5599–5608.

Rascle, N., Nouguier, F., Chapron, B., Mouche, A., & Ponte, A. (2016). Surface roughness changes by finescale current gradients: properties at multiple azimuth view angles. *Journal of Physical Oceanography*, *46*(12), 3681–3694.

Romero, L., Hypolite, D., & McWilliams, J. C. (2020). Submesoscale current effects on surface waves. *Ocean Modelling*, *153*, 101662.

Romero, L., Lenain, L., & Melville, W. K. (2017). Observations of surface wave–current interaction. *Journal of Physical Oceanography*, *47*(3), 615–632.

Schubert, R., Gula, J., Greatbatch, R. J., Baschek, B., & Biastoch, A. (2020). The submesoscale kinetic energy cascade: Mesoscale absorption of submesoscale mixed layer eddies and frontal downscale fluxes. *Journal of Physical Oceanography*, *50*(9), 2573–2589.

Shcherbina, A. Y., D'Asaro, E. A., Lee, C. M., Klymak, J. M., Molemaker, M. J., & McWilliams, J. C. (2013). Statistics of vertical vorticity, divergence, and strain in a developed submesoscale turbulence field. *Geophysical Research Letters*, *40*(17), 4706–4711.

Smeltzer, B. K., Æsøy, E., Ådnøy, A., & Ellingsen, S. Å. (2019). An improved method for determining near-surface currents from wave dispersion measurements. *Journal of Geophysical Research: Oceans*, *124*(12), 8832–8851.

Smith, K. M., Hamlington, P. E., & Fox-Kemper, B. (2016). Effects of submesoscale turbulence on ocean tracers. *Journal of Geophysical Research: Oceans*, *121*(1), 908–933.

Stern, M. E. (1965). Interaction of a uniform wind stress with a geostrophic vortex. In *Deep sea research and oceanographic abstracts* (Vol. 12, pp. 355–367).

Stewart, R. H., & Joy, J. W. (1974). Hf radio measurements of surface currents. In *Deep sea research and oceanographic abstracts* (Vol. 21, pp. 1039–1049).

Streßer, M., Carrasco, R., & Horstmann, J. (2017). Video-based estimation of surface currents using a low-cost quadcopter. *IEEE Geoscience and Remote Sensing Letters*, *14*(11), 2027–2031.

Su, Z., Wang, J., Klein, P., Thompson, A. F., & Menemenlis, D. (2018). Ocean submesoscales as a key component of the global heat budget. *Nature communications*, *9*(1), 1–8.
Sullivan, P. P., & McWilliams, J. C. (2010). Dynamics of winds and currents coupled to surface waves. *Annual Review of Fluid Mechanics*, *42*, 19-42.
Suzuki, N., & Fox-Kemper, B. (2016). Understanding stokes forces in the wave-averaged equations. *Journal of Geophysical Research: Oceans*, *121*(5), 3579–3596.
Thomas, M., Misra, S., Kambhamettu, C., & Kirby, J. T. (2005). A robust motion estimation algorithm for PIV. *Measurement Science and Technology*, *16*(3), 865.
Verma, V., & Sarkar, S. (2021). Lagrangian three-dimensional transport and dispersion by submesoscale currents at an upper-ocean front. *Ocean Modelling*, *165*, 101844.
Villas Bôas, A. B., Lenain, L., Cornuelle, B. D., Gille, S. T., & Mazloff, M. R. (2022). A broadband view of the sea surface height wavenumber spectrum. *Geophysical Research Letters*, *49*(4), e2021GL096699.
Vrećica, T., Pizzo, N., & Lenain, L. (2022). Observations of strongly modulated surface wave and wave breaking statistics at a submesoscale front. *Journal of Physical Oceanography*, *52*(2), 289 - 304. doi: 10.1175/JPO-D-21-0125.1
Wang, J., Dong, C., & Yu, K. (2020). The influences of the kuroshio on wave characteristics and wave energy distribution in the east china sea. *Deep Sea Research Part I: Oceanographic Research Papers*, *158*, 103228.
Wenegrat, J., & Arthur, R. (2018). Response of the atmospheric boundary layer to submesoscale sea surface temperature fronts. *Geophysical Research Letters*, *45*(24), 13–505.
Yuan, J., & Liang, J.-H. (2021). Wind-and wave-driven ocean surface boundary layer in a frontal zone: Roles of submesoscale eddies and ekman–stokes transport. *Journal of Physical Oceanography*, *51*(8), 2655–2680.

Airborne observations of surface winds, waves and currents from meso to submesoscales

Luc Lenain[1*], Benjamin K. Smeltzer[2,3], Nick Pizzo[1], Mara Freilich[1,4], Luke Colosi[1], Simen Å. Ellingsen[2], Laurent Grare[1], Hugo Peyriere[1], and Nick Statom[1]

[1]Scripps Institution of Oceanography, University of California San Diego, La Jolla, CA 92037, USA
[2]Department of Energy Process Engineering, Norwegian University of Science and Technology, N-7491 Trondheim, Norway
[3]SINTEF Ocean, Marinteknisk senter, N-7052 Trondheim, Norway
[4]Department of Earth, Environmnetal and Planetary Science and Division of Applied Mathematics, Brown University, Providence, RI 02912, USA

Key Points:

- Unique coincident and collocated airborne observations of SST, surface currents and properties of surface waves across submesoscales features
- A new airborne instrument enables observations of surface currents, vertical and horizontal shear to capture quickly evolving ocean features
- Such observations are crucial to develop better understanding of the physics of submesoscale processes and wave-current interaction

[*]Corresponding author: Luc Lenain llenain@ucsd.edu

Abstract
In this work we present a unique set of coincident and collocated high- resolution observations of surface currents and directional properties of surface waves collected from an airborne instrument, the Modular Aerial Sensing System (MASS), collected off the coast of Southern California. High-resolution observations of near surface current profiles and shear are obtained using a new instrument, DoppVis, capable of capturing horizontal spatial current variability down to 128m resolution. This data set provides a unique opportunity to examine how currents at scales ranging from 1-100 km modulate bulk (e.g. significant wave height), directional and spectral properties of surface gravity waves. Such observations are a step toward developing better understanding of the underlying physics of submesoscale processes (e.g. frontogenesis and frontal arrest) and the nature of transitions between mesoscale and submesoscale dynamics.

Plain Language Summary

In recent years, through improvement of computational resolution of global ocean models, scientists have begun to suspect that kilometer-scale eddies, whirlpools and fronts, called "submesoscale" variability, make important contributions to horizontal and vertical exchange of climate and biological variables in the upper ocean. Such features are challenging to analyze, because of their size (and how quickly they evolve; within hours), they are too large to study from a research vessel but smaller than regions typically studied with satellite measurements. In this work, we use a research aircraft instrumented to characterize ocean currents, temperature, color (in turn chlorophyll concentration) and the properties of surface waves over an area large enough to capture submesoscale processes. This approach is a step forward in understanding and quantifying the underlying physics of submesoscale processes, and in turn develops parameterization that can help improve the fidelity of weather and climate models.

1 Introduction

The transfer of mass, momentum, and energy between the atmosphere and ocean are complex due to their interactions across a broad range of space and time scales (Melville, 1996). A better understanding of the physics of these processes is fundamental for improved parameterizations used in coupled air-sea models of weather and climate, particularly as Earth's climate changes (Cavaleri et al., 2012). For example, although the importance of surface waves in these models has long been acknowledged, only relatively recently have global models included physics-based models of their effects (see, for example McWilliams & Restrepo, 1999; Sullivan & McWilliams, 2010; Li et al., 2016). Specifically, the effects of the non-breaking surface wave induced transport that catalyses Langmuir circulations have been shown to reduce errors in sea surface temperature (Belcher et al., 2012), crucial to climate modelling.

Submesoscale ocean currents have horizontal scales on the order of 0.1-10 km and have recently been hypothesized to make important contributions to vertical exchanges of climate and biological variables in the upper ocean as well as provide a pathway from energetically rich large scale flows to small scale dissipation. Model studies and limited observations (e.g. D'Asaro et al., 2018) show that submesoscale vertical exchange is concentrated near kilometer-scale fronts, jets, and eddies (McWilliams, 2016). Submesoscale physics are at the smallest scales that have been resolved in global ocean models, where their net effect on heat exchange between the ocean and atmosphere has shown to be much larger than mesoscale eddies (Su et al., 2018). However, these simulations are sensitive to the parameterized physics of the smaller scale motion, which remains poorly understood. To address the fundamental questions of the observed nature of submesoscale dynamics and the interactions between submesoscale dynamics and smaller scale surface wave processes, a comprehensive set of novel, coincident and collocated measurements of the dynamical variables is needed to improve state-of-the-art high-resolution simulations of weather and climate, and better understand vertical exchanges of heat and biogeochemical tracers.

Due to non-linear coupling between oceanic and atmospheric processes, including currents, winds, and waves, coincident observations are necessary to understand these dynamics. A number of model and observational studies have demonstrated the variety of ways by which air-sea interaction can induce horizontal divergence of surface currents and thus force vertical velocities. Coincident observations of surface vector winds and currents are needed to better understand the coupling of winds and currents and in turn improve surface flux parameterizations (Bourassa et al., 2019). The wind stress can be modified by SST and velocity gradients (Dewar & Flierl, 1987; Fairall et al., 1996; Chelton et al., 2004; O'Neill et al., 2005) while the resulting convergence of the ocean Ekman layer can be modified by surface vorticity (Stern, 1965; McGillicuddy Jr et al., 2007). At submesoscales, these effects are expected to increase in intensity. Frontal structures are strongly affected by the relative direction of the wind with *downfront* Ekman transport sharpening the fronts and inducing vertical exchange while *upfront* transport subdues the front and stratifies the upper ocean (Thomas et al., 2005). Surface waves and wave breaking can be strongly modulated at fronts (Romero et al., 2017; Vrećica et al., 2022), suggesting that even the basic formulation of air-sea exchange in terms of simple bulk coefficients will likely break down at sufficiently small scales. As such, an understanding of submesoscale structure and vertical velocity requires that air-sea interaction parameters be observed simultaneously with submesoscale measurements. Of particular interest are observations of surface and near surface currents, wave breaking (Vrećica et al., 2022), and the directional properties of ocean surface waves. While much progress have been made on characterizing the latter (e.g. Herbers et al., 2012; Lenain & Melville, 2014; Melville et al., 2016; Lenain & Melville, 2017; Lenain & Pizzo, 2020), collecting observations of near surface currents, i.e. from the surface down to several meters depth, remains challenging and spatially limited in large part due to the presence of waves, which induce platform motions and additional sources of background noise. An alternative approach to traditional in-situ techniques is to infer current profiles remotely based on observations of the spatio-temporal evolution of surface waves that follow a dispersion relationship, pursued in the present study.

In this work, we present a unique set of coincident and collocated observations of high-resolution surface currents and directional properties of surface waves collected from an airborne instrument, the Modular Aerial Sensing System (MASS), off the coast of Southern California in May 2021 as part of the ONR-funded Task Force Ocean (TFO) research initiative and in October 2021 as part of the NASA-funded Submesoscale Ocean Dynamics Experiment (S-MODE) research initiative. Two of the TFO research flights were dedicated to collecting observations across two small counter-rotating eddies separated by approximately 100 km. One of the S-MODE flights collected observations across a sharp SST front. This data set provides a unique opportunity to examine how currents at scales ranging from 1-100 km modulate surface gravity waves, i.e. bulk, directional and spectral properties.

This paper is structured as follows: the overview of the experiment and processing techniques is given in section 2 and 3. In sections 4 through 6, analysis of meso to submesoscales surface kinematics and currents collected during two experiments in Southern California is discussed. Section 7 discusses potential implications for submesoscale and air-sea interaction studies and presents some summary points.

2 Experiments

In this study we consider observations collected during two distinct experiments. The first was conducted as part of the "Platform Centric ASW Processing with Through-the-Sensor Data Assimilation and Fusion" project, funded through the ONR Task Force Ocean (TFO) initiative with the aim of collecting a simultaneous combination of acoustic, air-sea interaction and oceanographic measurements. Observations from a research vessel, a drifting instrument array, autonomous surface vehicles and a research aircraft were collected in May 2021, approximately 45km offshore of San Diego, CA, in the vicinity of CalCoFi Line #90.

The second experiment was conducted as part of the NASA S-MODE program, a project that aims to characterize the contribution of submesoscale ocean dynamics to vertical and horizontal transport in the upper ocean by employing a combination of aircraft-based remote sensing measurements of the ocean surface, in-situ measurements from research vessels and a variety of autonomous oceanographic platforms, and numerical modeling (Farrar et al., 2020). The "pilot" experiment considered here was conducted in the fall of 2021 off the coast of San Francisco, CA.

Data collected from instrumented Wave Gliders (Grare et al., 2021) and an airborne instrument, the SIO Modular Aerial Sensing System (MASS, Melville et al., 2016) during these two field programs are considered in the analysis. During both experiments the MASS instrument was installed on a Twin Otter DHC-6 aircraft (Twin Otter International, Grand Junction, CO).

3 SIO-MASS DoppVis instrument: Enabling novel airborne observations of near-surface currents

The Modular Aerial Sensing System (MASS) is an airborne instrument developed at the Air-Sea Interaction Laboratory (SIO) to simultaneously collect observations of sea surface temperature and ocean color (Melville et al., 2016; Lenain & Pizzo, 2021a), winds and mean-square slope (Lenain et al., 2019), surface waves (Lenain & Melville, 2017; Lenain & Pizzo, 2020), and ocean topography (Villas Bôas et al., 2022), at horizontal scales ranging from sub-meter to mesoscales. Over the past 11 years, the instrument was flown for more than 30 missions, covering a broad range of environmental conditions, locations, and applications. Details on the system performance and various applications of the MASS can be found in Melville et al. (2016); Lenain and Melville (2017); Lenain et al. (2019); Lenain and Pizzo (2020); Vrećica et al. (2022).

In 2020, we started the development and integration of a new sensor into the MASS instrument, called "DoppVis", to obtain coincident observations of surface currents alongside the MASS observations listed above. The approach used is to infer currents from optical observations of the spatio-temporal evolution of surface waves, whose dispersion is altered by the presence of an underlying current. This technique has been primarily used with radar technology (e.g. Stewart & Joy, 1974; Campana et al., 2016; Lund et al., 2015) then later applied to airborne video imagery (Dugan et al., 2001; Dugan & Piotrowski, 2003; Anderson et al., 2013).

Starting from the dispersion relation for small-amplitude linear waves propagating on top of a depth-varying current,

$$\omega(\mathbf{k}) = \omega_0(k) + \mathbf{c}(k) \cdot \mathbf{k}, \tag{1}$$

where ω is the wave frequency, ω_0 is the frequency in the absence of currents, i.e equal to $\sqrt{gk}$ in deep water, $\mathbf{k} = (k_x, k_y)$ is the wavenumber, $k = |\mathbf{k}|$, and $\mathbf{c}$ is the Doppler shift velocity due to the underlying current. Following Stewart and Joy (1974), assuming the waves are in deep-water, $\mathbf{c}$ can be approximated as a weighted average of the current profile as a function of depth such that

$$\mathbf{c}(k) = 2k \int_{-\infty}^{0} \mathbf{U}(z) e^{2kz} \mathrm{d}z, \tag{2}$$

where $\mathbf{U}(z) = (U, V)$ is the *Lagrangian* mean current profile as a function of depth z (Pizzo et al., 2022). Based on this relationship, one can assign an effective depth z_e to the measured Doppler velocities $\mathbf{c}(k)$ by finding the depth at which the Doppler velocity is equal to the current (Stewart & Joy, 1974; Smeltzer et al., 2019), such that $z_e(k) = -1/2k$. This is referred to as the Effective Depth Method (EDM) in Smeltzer et al. (2019).

The DoppVis instrument collects visible imagery of the ocean surface using a Nikon D850 camera with 14mm lens mounted with a 90 degree rotation (long edge of image parallel with flight track) and a 30 degree positive pitch angle from nadir (pointing slightly ahead of aircraft). The camera is synchronized to a coupled GPS/IMU system collecting images at a 2Hz frame rate. Raw images are carefully calibrated for lens distortion and boresight misalignment with the GPS/IMU over a hard terrestrial target, then georeferenced and exported with reference to WGS84 datum with a UTM zone 10 projection (EPSG 32610) at 50cm horizontal resolution. Each image is then interpolated on a regular grid, to enable the generation of 3D cubes of imagery (time, UTM X, UTM Y) of set duration and dimension (N_x, N_y), where $N_x = N_y$, typically in the range of 128 to 512m. The number of collected data cubes in the cross and along track direction of the aircraft varies as a function of aircraft altitude. All data presented here were collected at 1500 AMSL, corresponding to approximately two 256x256 m^2 cubes in the cross-track direction. Following the same approach described in (Smeltzer et al., 2019), all cubes of space–time data are converted to wavenumber–frequency space using a 3D FFT. Each of these 3D spectra are then averaged in the cross-track and along-track direction (1 km bin) to improve SNR. Doppler shift velocities are extracted from the spectrum as a function of wavenumber by masking the spectrum into wavenumber magnitude bins (bin half-width of $4\pi/N_x$), where for each bin the current $\mathbf{c}(k)$ is estimated using a normalized scalar product method (Huang et al., 2016; Streßer et al., 2017) with a Gaussian characteristic function (Smeltzer et al., 2019) peaked along the linear dispersion relation.

Figure 1(a) shows an example of current profiles (U, V) collected from DoppVis during an overflight of an instrumented Wave Glider during the S-MODE experiment on November 4, 2021 at 17:20 UTC. The Wave Glider was instrumented with an upward-looking Nortek Signature 1000 ADCP (orange squares) and a downward-looking ADCP (Teledyne RDI Workhorse 300kHz), carefully motion compensated using an onboard GPS/IMU system (Grare et al., 2021). Observations from DoppVis and the wave glider were collected within 5min and no further than 500m from each other to minimize any error associated with natural spatial and temporal variability. We find good agreement between in-situ and remotely sensed observations of near-surface current (U, V), with a bias = -0.014 m/s and rms deviation = 0.052 m/s, and a coefficient of determination $R^2 = 0.96$.

Finally, airborne observations of SST collected from MASS on November 4, 2021, over the entire domain along with current estimates (1km along-track resolution) from DoppVis at two depths, $z = -1.5 \pm 0.5$m (black arrows) and $z = -0.4 \pm 0.1$m (red arrows) are shown in figure 1(c). Note the correlation between features present in the SST fields and the surface currents from DoppVis. Throughout the domain, we consistently find larger magnitudes of the eastern component of the current closer to the surface, likely caused by Stokes drift included in the Lagrangian current observed by DoppVis (Pizzo et al., 2022). Wind and waves were coming from the west at the time of the flight.

4 Wave-current interactions from meso- to submesoscales

The collocated observations from the multiple instruments on the MASS allow for investigation of interactions between currents and other oceanographic properties such as waves, heat, and biological communities. We now examine observations collected during the "Platform Centric ASW Processing with Through-the-Sensor Data Assimilation and Fusion" TFO project in May 2021 to illustrate the importance of high spatial resolution, collocated observations for studying wave-current observations.

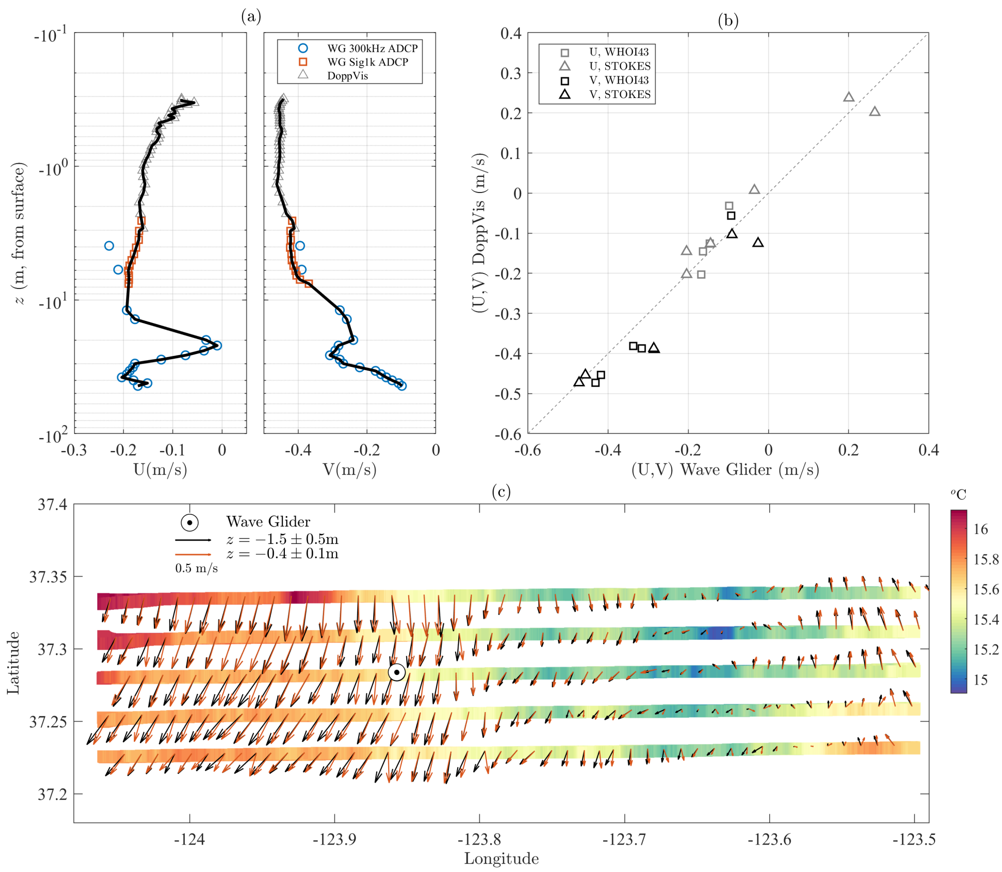

Figure 1. (a) Current profiles (U, V) collected from DoppVis (gray triangles) during an overflight of an instrumented Wave Glider during the S-MODE experiment on November 4, 2021 at 17:20 UTC. The Wave Glider is equipped with an upward-looking Nortek Signature 1000 ADCP (orange squares) and a downward-looking ADCP (Teledyne RDI Workhorse 300kHz; blue circles). The location of the Wave Glider with respect to the DoppVis observations is shown in (c). (b) Comparison between in-situ observations of currents collected at a 2 to 3m water depth obtained from DoppVis and two Wave Gliders, named WHOI43 and STOKES, for the times and locations of overflights (within 500m) during the entire S-MODE experiment. (c) Airborne observations of SST collected from MASS on November 4, 2021 over the entire domain along with current estimates (1km along-track resolution) from DoppVis at two depths, deep, $z = -1.5 \pm 0.5$m (black arrows) and shallow, $z = -0.4 \pm 0.1$m (red arrows).

Several research flights were dedicated to collecting observations across two counter-rotating eddies separated by approximately 100 km. Figure 2(a) shows depth-averaged (0.3-2m) surface currents (250 m along-track resolution) along with significant wave height measurements collected coincidentally with the MASS instrument. The black contours represent the sea surface height (ssh, AVISO) at the time of the observations, while corresponding surface currents from HYCOM (GOF 3.1, GLBy0.08-expt93.0) are shown as gray quivers. We find the HYCOM estimated currents to be in good agreement with DoppVis observations at the mesoscale, but strikingly miss many of the submesoscale features throughout the domain. We also find significant modulation of the surface wave properties across the domain that is not caused by temporal (e.g. inertial) variability.

Currents modulate the properties of surface gravity waves both through wave refraction (e.g. Ardhuin et al., 2017; Romero et al., 2017, 2020; Bôas et al., 2020; Pizzo & Salmon, 2021) and local effects (Rascle et al., 2016, 2017; Lenain & Pizzo, 2021b), therefore high-resolution measurements of currents and spectral wave properties is needed to better understand wave-current interaction from meso- to submesoscales.

Figure 2 shows a subset of these observations, focusing on an area of the domain with significant submesoscale variability in ocean current magnitude and direction. We find large modulation of surface currents, at scales of 1-8 km associated with submesoscale variations within the mesoscale eddy. Panel (b) shows a sharp SST front at 32.885^{o}N with a change in temperature of approximately 0.5^oC, associated with a velocity gradient $\partial U/\partial x \approx 10f$, where f is the Coriolis frequency.

Despite approximately constant surface wind (figure 2c) and significant wave height (figure 2d) as a function of latitude on this transect, the mean spectral saturation $< B >$ (Romero et al., 2017) had significant variation (figure 2e). The saturation spectrum is defined as $B = \phi(k)k^3$, where ϕ is the omnidirectional wave spectrum (Phillips, 1984, 1985). The mean saturation is obtained by averaging B over the saturation range of the wave spectrum, with a lower bound k_n as defined in Lenain and Pizzo (2020). At that time, wind waves were approximately oriented in the same direction as the current V (figure 2d).

We find that the mean saturation $< B >$ generally follow the same evolution as V. While this comparison remains qualitative, it hints at the importance of incorporating wave-current interaction in wave spectrum parameterization, along the line of Lenain and Pizzo (2021a) that investigated the use of WKB to predict the modulation of surface gravity waves by internal wave currents.

Though beyond the scope of this work, but a focus of further studies in particular as part of the S-MODE program, we expect that these collocated, coincident observations will lead to new insights about coherent features that arise from wind-wave-current coupling, or some combination of those processes, which may be particularly important for the flux of climatically-important variables such as heat and biogeochemical tracers between atmosphere and ocean (Li et al., 2016; Smith et al., 2016; Verma & Sarkar, 2021; Freilich & Mahadevan, 2021; Gula et al., 2022).

5 Transitions from mesoscale to submesoscale motion

High-resolution measurements of surface currents enable the characterization of the transition between geostrophically balanced motion at larger scales and unbalanced (ageostrophic and wave) motion at smaller scales (Chereskin et al., 2019). In particular, determining the dynamics that predominate at the submesoscale has important implications for the vertical structure of the upper-ocean (Cronin et al., 2019) and the spatio-temporal distribution of energy dissipation (Buckingham et al., 2019; Dong et al., 2020; Schubert et al., 2020; Ajayi et al., 2021), and can lead to improvement of ocean-atmosphere coupled models (Li et al., 2016). While DoppVis observations are accurate enough to resolve sub-

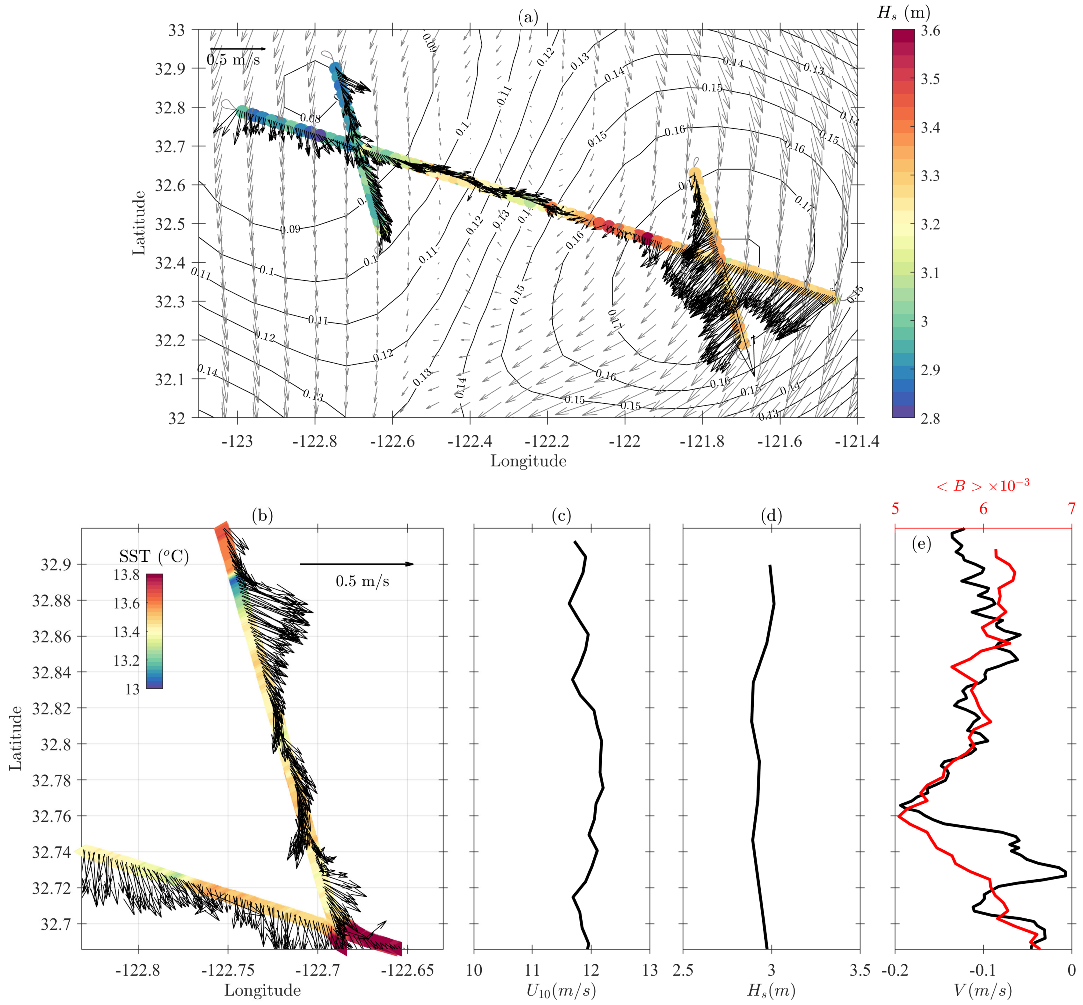

Figure 2. (a) MASS significant wave height H_s and DoppVis surface current observations (250m along-track resolution) collected during the TFO experiment on May 19, 2021. The black contours represent the sea surface height (ssh, AVISO) at the time of the observations, while corresponding surface currents from HYCOM are shown as gray quivers. The larger scale trends of the surface currents are in general agreement with the HYCOM product, though the latter completely misses significant submesoscale features. We find significant modulation of the wave conditions across the domain, by up to 20%. (b) Subset of the data presented in (a) (nortwestern part of the flight) with the track colorcoded for measured SST. Note the strong modulation of surface currents over very short distances (1-8 km), coinciding in places with sharp SST fronts (for example at latitude around 32.885^o in the northern part of the operation area). (c) and (d) show the wind speed U_{10} and significant wave height H_s collected along the NNW-SSE track shown in panel (b). (e) North component of the current V and mean spectral saturation $\langle B \rangle$, all plotted over the same range of latitude as in panel (b). Note the modulation of $\langle B \rangle$ associated with changes in V, the component of the current aligned with the waves, hinting at local wave-current interaction.

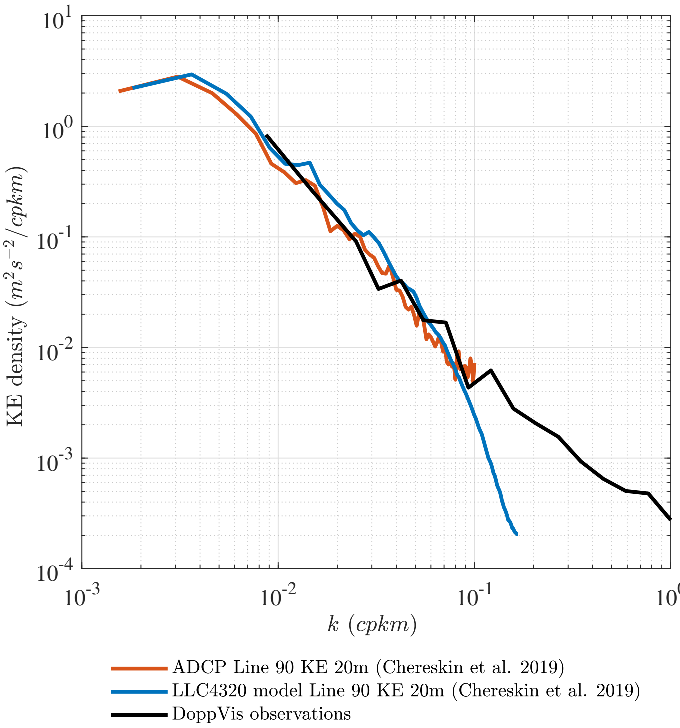

Figure 3. Comparison of Kinetic energy (KE) spectra collected from the DoppVis Lagrangian surface currents on May 19 2021 during one of the long East - West transects shown in figure 2(a) compared with in-situ ADCP observations (20-m depth) and LLC4320 hourly model products from Chereskin et al. (2019).

mesoscale currents (horizontal resolution of less than 500 m), the airborne platform also travels quickly enough to collect nearly synoptic observations at the mesoscale (100 km). This is particularly valuable because it allows for examination of spatial variability across a range of scales and cross-scale interactions by not aliasing temporal variability. Figure 3 shows kinetic energy (KE) spectra computed from the DoppVis surface current observations collected during one of the long East-West transects shown in figure 2(a) compared with the average of 11 years of in-situ ADCP observations (20-m depth) and 1 year of LLC4320 hourly model products from Chereskin et al. (2019). The agreement at low wavenumbers (>10km) is remarkable, as well as the fact that the kinetic energy spectrum from DoppVis maintains a nearly continuous slope for higher wavenumbers, down to 1 km scale. Feedbacks on ocean currents from wind and waves is likely important for determining dynamics at scales of less than 10 km where submesoscale processes predominate (Haney et al., 2015; Suzuki & Fox-Kemper, 2016; Yuan & Liang, 2021). Understanding these couplings needs to be advanced by direct observations that span scales from submesoscale to mesoscale. Characterization of the transition between geostrophically balanced motion and unbalanced dynamics is further explored in forthcoming work.

6 Velocity gradient statistics

Submesoscale dynamics are defined by the large velocity gradients at these scales, with $\mathcal{O}(1)$ Rossby number (McWilliams, 2016). Consistent with the small spatial scale of submesoscale dynamics, they also have fast temporal scales (Callies et al., 2020). Observations of not just velocity, but 2D velocity gradients of quickly evolving submesoscale features are therefore important for understanding submesoscale dynamics, but require

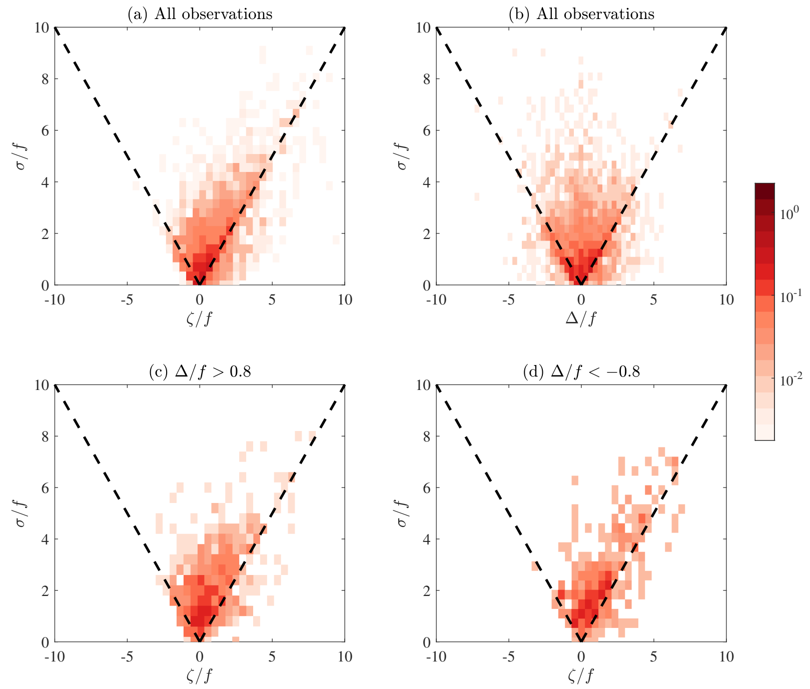

Figure 4. (a) Surface vorticity–strain and (b) divergence-strain JPDFs computed from 128m resolution DoppVis products collected on October 5 2021 during the S-MODE pilot program. (c) and (d) Surface vorticity–strain for $\Delta/f > 0.8$ and $\Delta/f < -0.8$ respectively. The dashed lines represents the $\sigma = \zeta$ lines.

synoptic observations over scales of tens of kilometers, which is not feasible with relatively slow-moving ship-based observations. Previous observations of submesoscale velocity gradients have used two ships (Shcherbina et al., 2013). Aircraft-based observations offer a well-suited platform for studying submesoscale dynamics due to their fast speed relative to ships and much higher resolution measurements than what is afforded by satellites.

In recent years, through numerical (Balwada et al., 2021) and observational (Shcherbina et al., 2013) studies, the surface vorticity–strain Joint Probability Density Function (JPDF) has been demonstrated as a useful tool to distinguish between different flow regimes, in particular in the context of submesoscale dynamics. In figure 4, we show vorticity-strain and divergence-strain JPDFs computed from high-resolution DoppVis surface current observations collected during the S-MODE pilot experiment on October 2021 (60km long section). During that portion of the flight, the aircraft flew at 3000ft AMSL, increasing the swath width of surface current observation up to 2 km, with a horizontal resolution (cross and along-track) of 128 m. Vorticity ζ, strain rate σ and divergence Δ are then computed from the gradients of the measured surface currents. These velocities are first low-pass filtered (3-point tophat) prior to computing gradients. Overall, the distribution is skewed toward positive ζ/f values, with $\sigma/f > \zeta/f$ consistent with frontal structures, and classical submesoscale frontogenesis. This is particularly evident in panel (d), where the vorticity-strain JPDF for $\Delta/f < -0.8$ (i.e. convergence) is shown to be skewed to positive values. The same JPDF for positive values of Δ/f, larger than 0.8 (panel c) is not skewed toward negative ζ/f values, perhaps implying the contribution of other processes, e.g. surface wave modulation properties and associated Stokes drift (recall that DoppVis observes Lagrangian current).

7 Discussions and summary

Direct spatial and temporal observations of the lower atmosphere, sea surface and upper ocean are crucial for improved knowledge of air-sea interaction. However, the broad range of scales, or equivalently the strong spatial and temporal variability of theses interactions (see figure 1), make this a formidable theoretical, numerical, and observational challenge. Traditional in-situ assets such as moorings and buoys are limited by their spatial coverage or their potential spatial biasing, in particular near an ocean front where buoys or drifters can cluster, while satellite imagery estimates important quantities like wind, significant wave height and currents through indirect methods (often based on σ_0 relations) and can also only sample at sparse time intervals. Observations and models have revealed two-way coupling processes between ocean currents and wind (Chelton & Xie, 2010; Wenegrat & Arthur, 2018) and ocean currents and waves (Marechal & de Marez, 2022; Wang et al., 2020) at both the mesoscale and submesoscale.

In this work, we present unique coincident and collocated suborbital high-resolution observations of SST, surface currents and directional properties of surface waves collected from an airborne instrument (MASS), off the coast of Southern California, across submesoscales features.

Central to this work is the development of a novel airborne instrument, DoppVis, that enables high-resolution observations of surface currents, vertical and horizontal shear alongside the other MASS instruments to capture quickly evolving features (both in time and space) such as submesoscale fronts, but also tidal estuarine flows, and more generally ocean phenomena that require frequent revisits (e.g oil spills).

The combination of surface waves, currents, and SST remotely observed from this instrument provides a unique opportunity to examine how currents at scales ranging from 1-100 km modulate surface gravity waves, i.e. bulk (e.g. significant wave height), directional and spectral properties. Observations of near-surface currents at such high spatial resolution also enable the investigation of the transition between balanced and unbalanced motion, and the flow structure (vorticity-strain space), crucial to developing a better understanding of the underlying physics of submesoscale processes such as frontogenesis and frontal arrest.

Acknowledgments

We gratefully acknowledge useful comments from Ernesto Rodriguez and Roy Barkan. The authors are grateful to Twin Otter International for providing flight resources. This research was supported by grants from the Physical Oceanography programs at ONR (Grant N00014-19-1-2635), and NASA (Grant 80NSSC19K1688).

Open research

Data availability: All presented data will be found at the UCSD Library Digital Collection, https://doi.org/10.6075/J0F76CRK (data archiving is underway).

References

Ajayi, A., Le Sommer, J., Chassignet, E. P., Molines, J.-M., Xu, X., Albert, A., & Dewar, W. (2021). Diagnosing cross-scale kinetic energy exchanges from two submesoscale permitting ocean models. *Journal of Advances in Modeling Earth Systems*, *13*(6), e2019MS001923.

Anderson, S. P., Zuckerman, S., Fan, S., & van Smirren, J. (2013). Airborne optical remote sensing of ocean currents. In *2013 oceans-san diego* (pp. 1–7).

Ardhuin, F., Gille, S. T., Menemenlis, D., Rocha, C. B., Rascle, N., Chapron, B.,

... Molemaker, J. (2017). Small-scale open ocean currents have large effects on wind wave heights. *Journal of Geophysical Research: Oceans*, *122*(6), 4500–4517.

Balwada, D., Xiao, Q., Smith, S., Abernathey, R., & Gray, A. R. (2021). Vertical fluxes conditioned on vorticity and strain reveal submesoscale ventilation. *Journal of Physical Oceanography*, *51*(9), 2883–2901.

Belcher, S. E., Grant, A. L., Hanley, K. E., Fox-Kemper, B., Van Roekel, L., Sullivan, P. P., ... others (2012). A global perspective on langmuir turbulence in the ocean surface boundary layer. *Geophysical Research Letters*, *39*(18).

Bôas, A. B. V., Cornuelle, B. D., Mazloff, M. R., Gille, S. T., & Ardhuin, F. (2020). Wave–current interactions at meso-and submesoscales: Insights from idealized numerical simulations. *Journal of Physical Oceanography*, *50*(12), 3483–3500.

Bourassa, M. A., Meissner, T., Cerovecki, I., Chang, P. S., Dong, X., De Chiara, G., ... others (2019). Remotely sensed winds and wind stresses for marine forecasting and ocean modeling. *Frontiers in Marine Science*, 443.

Buckingham, C. E., Lucas, N. S., Belcher, S. E., Rippeth, T. P., Grant, A. L., Le Sommer, J., ... Naveira Garabato, A. C. (2019). The contribution of surface and submesoscale processes to turbulence in the open ocean surface boundary layer. *Journal of Advances in Modeling Earth Systems*, *11*(12), 4066–4094.

Callies, J., Barkan, R., & Garabato, A. N. (2020). Time scales of submesoscale flow inferred from a mooring array. *Journal of Physical Oceanography*, *50*(4), 1065–1086.

Campana, J., Terrill, E. J., & De Paolo, T. (2016). The development of an inversion technique to extract vertical current profiles from x-band radar observations. *Journal of Atmospheric and Oceanic Technology*, *33*(9), 2015–2028.

Cavaleri, L., Fox-Kemper, B., & Hemer, M. (2012). Wind waves in the coupled climate system. *Bulletin of the American Meteorological Society*, *93*(11), 1651–1661.

Chelton, D. B., Schlax, M. G., Freilich, M. H., & Milliff, R. F. (2004). Satellite measurements reveal persistent small-scale features in ocean winds. *science*, *303*(5660), 978–983.

Chelton, D. B., & Xie, S.-P. (2010). Coupled ocean-atmosphere interaction at oceanic mesoscales. *Oceanography*, *23*(4), 52–69.

Chereskin, T. K., Rocha, C. B., Gille, S. T., Menemenlis, D., & Passaro, M. (2019). Characterizing the transition from balanced to unbalanced motions in the southern california current. *Journal of Geophysical Research: Oceans*, *124*(3), 2088–2109.

Cronin, M. F., Gentemann, C. L., Edson, J., Ueki, I., Bourassa, M., Brown, S., ... others (2019). Air-sea fluxes with a focus on heat and momentum. *Frontiers in Marine Science*, *6*, 430.

Dewar, W. K., & Flierl, G. R. (1987). Some effects of the wind on rings. *Journal of physical oceanography*, *17*(10), 1653–1667.

Dong, J., Fox-Kemper, B., Zhang, H., & Dong, C. (2020). The seasonality of submesoscale energy production, content, and cascade. *Geophysical Research Letters*, *47*(6), e2020GL087388.

Dugan, J., & Piotrowski, C. (2003). Surface current measurements using airborne visible image time series. *Remote Sensing of Environment*, *84*(2), 309–319.

Dugan, J., Piotrowski, C., & Williams, J. (2001). Water depth and surface current retrievals from airborne optical measurements of surface gravity wave dispersion. *Journal of Geophysical Research: Oceans*, *106*(C8), 16903–16915.

D'Asaro, E. A., Shcherbina, A. Y., Klymak, J. M., Molemaker, J., Novelli, G., Guigand, C. M., ... others (2018). Ocean convergence and the dispersion of flotsam. *Proceedings of the National Academy of Sciences*, *115*(6), 1162–1167.

Fairall, C. W., Bradley, E. F., Rogers, D. P., Edson, J. B., & Young, G. S. (1996). Bulk parameterization of air-sea fluxes for tropical ocean-global atmosphere coupled-ocean atmosphere response experiment. *Journal of Geophysical Research: Oceans*, *101* (C2), 3747–3764.

Farrar, J. T., D'Asaro, E., Rodriguez, E., Shcherbina, A., Czech, E., Matthias, P., ... others (2020). S-mode: The sub-mesoscale ocean dynamics experiment. In *Igarss 2020-2020 ieee international geoscience and remote sensing symposium* (pp. 3533–3536).

Freilich, M., & Mahadevan, A. (2021). Coherent pathways for subduction from the surface mixed layer at ocean fronts. *Journal of Geophysical Research: Oceans*, *126* (5), e2020JC017042.

Grare, L., Statom, N. M., Pizzo, N., & Lenain, L. (2021). Instrumented wave gliders for air-sea interaction and upper ocean research. *Frontiers in Marine Science*, 888.

Gula, J., Taylor, J., Shcherbina, A., & Mahadevan, A. (2022). Submesoscale processes and mixing. In *Ocean mixing* (pp. 181–214). Elsevier.

Haney, S., Fox-Kemper, B., Julien, K., & Webb, A. (2015). Symmetric and geostrophic instabilities in the wave-forced ocean mixed layer. *Journal of Physical Oceanography*, *45* (12), 3033–3056.

Herbers, T. H. C., Jessen, P. F., Janssen, T. T., Colbert, D. B., & MacMahan, J. H. (2012). Observing ocean surface waves with gps-tracked buoys. *J. Atmos. Oceanic Technol.*, *29*, 944–959.

Huang, W., Carrasco, R., Shen, C., Gill, E. W., & Horstmann, J. (2016). Surface current measurements using x-band marine radar with vertical polarization. *IEEE Transactions on Geoscience and Remote Sensing*, *54* (5), 2988–2997.

Lenain, L., & Melville, W. K. (2014). Autonomous surface vehicle measurements of the ocean's response to tropical cyclone freda. *Journal of Atmospheric and Oceanic Technology*, *31* (10), 2169–2190.

Lenain, L., & Melville, W. K. (2017). Measurements of the directional spectrum across the equilibrium saturation ranges of wind-generated surface waves. *Journal of Physical Oceanography*, *47* (8), 2123–2138.

Lenain, L., & Pizzo, N. (2020, 09). The contribution of high frequency wind-generated surface waves to the Stokes drift. *Journal of Physical Oceanography*, 1-39. Retrieved from `https://doi.org/10.1175/JPO-D-20-0116.1` doi: 10.1175/JPO-D-20-0116.1

Lenain, L., & Pizzo, N. (2021a). Modulation of surface gravity waves by internal waves. *Journal of Physical Oceanography*, *51* (9), 2735–2748.

Lenain, L., & Pizzo, N. (2021b). Modulation of surface gravity waves by internal waves. *Journal of Physical Oceanography*, *51* (9), 2735–2748.

Lenain, L., Statom, N. M., & Melville, W. K. (2019). Airborne measurements of surface wind and slope statistics over the ocean. *Journal of Physical Oceanography*(2019).

Li, Q., Webb, A., Fox-Kemper, B., Craig, A., Danabasoglu, G., Large, W. G., & Vertenstein, M. (2016). Langmuir mixing effects on global climate: Wavewatch iii in cesm. *Ocean Modelling*, *103*, 145–160.

Lund, B., Graber, H. C., Tamura, H., Collins III, C., & Varlamov, S. (2015). A new technique for the retrieval of near-surface vertical current shear from marine x-band radar images. *Journal of Geophysical Research: Oceans*, *120* (12), 8466–8486.

Marechal, G., & de Marez, C. (2022). Variability of surface gravity wave field over a realistic cyclonic eddy. *Ocean Science*, *18* (5), 1275–1292.

McGillicuddy Jr, D. J., Anderson, L. A., Bates, N. R., Bibby, T., Buesseler, K. O., Carlson, C. A., ... others (2007). Eddy/wind interactions stimulate extraordinary mid-ocean plankton blooms. *Science*, *316* (5827), 1021–1026.

McWilliams, J. C. (2016). Submesoscale currents in the ocean. *Proceedings of the*

Royal Society A: Mathematical, Physical and Engineering Sciences, *472*(2189), 20160117.

McWilliams, J. C., & Restrepo, J. M. (1999). The wave-driven ocean circulation. *Journal of Physical Oceanography*, *29*(10), 2523–2540.

Melville, W. K. (1996). The role of surface wave breaking in air-sea interaction. *Annual Review of Fluid Mechanics*, *28*, 279-321.

Melville, W. K., Lenain, L., Cayan, D. R., Kahru, M., Kleissl, J. P., Linden, P., & Statom, N. M. (2016). The modular aerial sensing system. *Journal of Atmospheric and Oceanic Technology*, *33*(6), 1169–1184.

O'Neill, L. W., Chelton, D. B., Esbensen, S. K., & Wentz, F. J. (2005). High-resolution satellite measurements of the atmospheric boundary layer response to sst variations along the agulhas return current. *Journal of Climate*, *18*(14), 2706 - 2723. doi: 10.1175/JCLI3415.1

Phillips, O. (1984). On the response of short ocean wave components at a fixed wavenumber to ocean current variations. *Journal of Physical Oceanography*, *14*(9), 1425–1433.

Phillips, O. (1985). Spectral and statistical properties of the equilibrium range in wind-generated gravity waves. *Journal of Fluid Mechanics*, *156*(1), 505–31.

Pizzo, N., Lenain, L., Romcke, O., Ellingsen, O., & Smeltzer, B. (2022). The role of lagrangian drift in the geometry, kinematics and dynamics of surface waves. *Journal of Fluid Mechanics*, *Sub Judice*.

Pizzo, N., & Salmon, R. (2021). Particle description of the interaction between wave packets and point vortices. *Journal of Fluid Mechanics*, *925*.

Rascle, N., Molemaker, J., Marié, L., Nouguier, F., Chapron, B., Lund, B., & Mouche, A. (2017). Intense deformation field at oceanic front inferred from directional sea surface roughness observations. *Geophysical Research Letters*, *44*(11), 5599–5608.

Rascle, N., Nouguier, F., Chapron, B., Mouche, A., & Ponte, A. (2016). Surface roughness changes by finescale current gradients: properties at multiple azimuth view angles. *Journal of Physical Oceanography*, *46*(12), 3681–3694.

Romero, L., Hypolite, D., & McWilliams, J. C. (2020). Submesoscale current effects on surface waves. *Ocean Modelling*, *153*, 101662.

Romero, L., Lenain, L., & Melville, W. K. (2017). Observations of surface wave–current interaction. *Journal of Physical Oceanography*, *47*(3), 615–632.

Schubert, R., Gula, J., Greatbatch, R. J., Baschek, B., & Biastoch, A. (2020). The submesoscale kinetic energy cascade: Mesoscale absorption of submesoscale mixed layer eddies and frontal downscale fluxes. *Journal of Physical Oceanography*, *50*(9), 2573–2589.

Shcherbina, A. Y., D'Asaro, E. A., Lee, C. M., Klymak, J. M., Molemaker, M. J., & McWilliams, J. C. (2013). Statistics of vertical vorticity, divergence, and strain in a developed submesoscale turbulence field. *Geophysical Research Letters*, *40*(17), 4706–4711.

Smeltzer, B. K., Æsøy, E., Ådnøy, A., & Ellingsen, S. Å. (2019). An improved method for determining near-surface currents from wave dispersion measurements. *Journal of Geophysical Research: Oceans*, *124*(12), 8832–8851.

Smith, K. M., Hamlington, P. E., & Fox-Kemper, B. (2016). Effects of submesoscale turbulence on ocean tracers. *Journal of Geophysical Research: Oceans*, *121*(1), 908–933.

Stern, M. E. (1965). Interaction of a uniform wind stress with a geostrophic vortex. In *Deep sea research and oceanographic abstracts* (Vol. 12, pp. 355–367).

Stewart, R. H., & Joy, J. W. (1974). Hf radio measurements of surface currents. In *Deep sea research and oceanographic abstracts* (Vol. 21, pp. 1039–1049).

Streßer, M., Carrasco, R., & Horstmann, J. (2017). Video-based estimation of surface currents using a low-cost quadcopter. *IEEE Geoscience and Remote Sensing Letters*, *14*(11), 2027–2031.

Su, Z., Wang, J., Klein, P., Thompson, A. F., & Menemenlis, D. (2018). Ocean submesoscales as a key component of the global heat budget. *Nature communications*, *9*(1), 1–8.

Sullivan, P. P., & McWilliams, J. C. (2010). Dynamics of winds and currents coupled to surface waves. *Annual Review of Fluid Mechanics*, *42*, 19-42.

Suzuki, N., & Fox-Kemper, B. (2016). Understanding stokes forces in the wave-averaged equations. *Journal of Geophysical Research: Oceans*, *121*(5), 3579–3596.

Thomas, M., Misra, S., Kambhamettu, C., & Kirby, J. T. (2005). A robust motion estimation algorithm for PIV. *Measurement Science and Technology*, *16*(3), 865.

Verma, V., & Sarkar, S. (2021). Lagrangian three-dimensional transport and dispersion by submesoscale currents at an upper-ocean front. *Ocean Modelling*, *165*, 101844.

Villas Bôas, A. B., Lenain, L., Cornuelle, B. D., Gille, S. T., & Mazloff, M. R. (2022). A broadband view of the sea surface height wavenumber spectrum. *Geophysical Research Letters*, *49*(4), e2021GL096699.

Vrećica, T., Pizzo, N., & Lenain, L. (2022). Observations of strongly modulated surface wave and wave breaking statistics at a submesoscale front. *Journal of Physical Oceanography*, *52*(2), 289 - 304. doi: 10.1175/JPO-D-21-0125.1

Wang, J., Dong, C., & Yu, K. (2020). The influences of the kuroshio on wave characteristics and wave energy distribution in the east china sea. *Deep Sea Research Part I: Oceanographic Research Papers*, *158*, 103228.

Wenegrat, J., & Arthur, R. (2018). Response of the atmospheric boundary layer to submesoscale sea surface temperature fronts. *Geophysical Research Letters*, *45*(24), 13–505.

Yuan, J., & Liang, J.-H. (2021). Wind-and wave-driven ocean surface boundary layer in a frontal zone: Roles of submesoscale eddies and ekman–stokes transport. *Journal of Physical Oceanography*, *51*(8), 2655–2680.